

## EVIDENCE FOR A BLACK HOLE IN THE X-RAY BINARY NOVA MUSCAE 1991

RONALD A. REMILLARD<sup>1</sup>

Center for Space Research, Massachusetts Institute of Technology, Cambridge, MA 02139

JEFFREY E. MCCLINTOCK<sup>1</sup>

Harvard-Smithsonian Center for Astrophysics, 60 Garden Street, Cambridge, MA 02138

AND

CHARLES D. BAILYN<sup>1</sup>

Department of Astronomy, Yale University, P.O. Box 6666, New Haven, CT 06511

Received 1992 May 26; accepted 1992 August 24

### ABSTRACT

Optical photometry and spectroscopy of the X-ray Nova Muscae 1991 in quiescence reveal an orbital period of  $10.398 \pm 0.014$  hr and an absorption-line velocity curve consistent with a sinusoidal modulation at a half-amplitude of  $409 \pm 18$  km s<sup>-1</sup>. The spectral type of the secondary star is in the range K0 V to K4 V. The value of the mass function,  $3.1 \pm 0.4 M_{\odot}$ , is a conservative lower limit on the mass of the compact primary and suggests that the primary is a black hole. Further considerations of the binary inclination angle and the mass of the secondary strengthen the black hole model. The folded light curves in the *I* band and the *B+V* band resemble ellipsoidal variations, with an additional brightening near one of the maxima in the *B+V* band. The orbital period is 1.4% shorter than the photometric period observed during outburst, as expected if the outburst modulations are analogs of “superhumps” in dwarf novae. In quiescence, the optical properties of the X-ray binary Nova Muscae 1991 bear a striking resemblance to the black hole binary A0620–00 (Nova Mon 1917, 1975), which extends the basis of similarity that was demonstrated during outburst at X-ray and optical wavelengths.

*Subject headings:* binaries: spectroscopic — black hole physics — X-rays: stars

### 1. INTRODUCTION

The measurement of the radial velocity of the secondary star in an X-ray binary system is a primary means of probing the masses of accreting neutron stars and black holes. Evidence for stellar-mass black holes has depended exclusively on studies of X-ray sources such as Cyg X-1 (Bolton 1975) and LMC X-3 (Cowley et al. 1983), which have massive (early-type) companions, and A0620–00 (McClintock & Remillard 1986) and V404 Cyg (Casares, Charles, & Naylor 1992), which have low-mass (late-type) companions. It is seldom possible to observe the secondary star in a low-mass X-ray binary (LMXB) because the X-ray-illuminated accretion disk is normally much brighter than the secondary. In a quiescent X-ray nova, however, the secondary can, in principle, be observed. Those nova-type LMXBs that are bright enough for spectral observations during quiescence are quite rare, yet they provide a wealth of information about the binary constituents. In the case of A0620–00 and V404 Cyg (see references above), the measured mass function alone is too large for models of stable neutron stars. This condition, namely a system with a compact-object mass that exceeds the upper limit for a neutron star ( $\sim 3 M_{\odot}$ ), serves as an operational definition that governs our use of the term “black hole” (cf. McClintock & Remillard 1986 and references therein).

There are other measurement tools for investigating compact objects in X-ray binaries. The light curve produced by the gravity-distorted secondary star seen at different orientations (“ellipsoidal variations”) can be modeled to constrain the

binary inclination angle and the mass ratio (e.g., Avni 1978; McClintock & Remillard 1990). Additional constraints may be derived via analysis of the widths of absorption lines of the secondary (e.g., Gies & Bolton 1986) and analyses of broad H $\alpha$  emission from a residual accretion disk (e.g., Johnston, Kulkarni, & Oke 1989; Haswell & Shafer 1990; Casares & Charles 1992).

The X-ray binary Nova Muscae 1991 (hereafter XN Mus 1991) was discovered independently by the WATCH/*Granat* instrument and the *Ginga* All-Sky X-Ray Monitor on 1991 January 9 (Lund & Brandt 1991; Makino et al. 1991). A coincident optical nova ( $V \sim 13$ ) was soon discovered at a position normally occupied by a star of brightness  $R = 19.4$  and  $B = 20.9$  (Della Valle, Jarvis, & West 1991a). During the outburst decay, Bailyn (1992) discovered a 10.5 hr optical modulation. The narrow optical maxima in the folded light curves were devoid of color variations, and they changed in shape on a time scale of days. The results were interpreted as the precession of an elliptical accretion disk on a time scale near the orbital period, analogous to the “superhump” phenomenon in cataclysmic variables. Bailyn’s prediction of an orbital period slightly shorter than 10.5 hr is confirmed in § 4 below.

The observations of XN Mus 1991 during outburst prompted frequent comparisons with A0620–00 (e.g., Della Valle, Jarvis, & West 1991b; Sunyaev et al. 1992) based on the nova decay time scale, the two-component X-ray spectrum, the observation of a radio nova (Kesteven & Turtle 1991), the amplitude and spectrum of the optical outburst, and evidence for an orbital period indicative of an LMXB. Cheng et al. (1992) observed XN Mus 1991 with the *Hubble Space Telescope* during outburst. They determined a color excess

<sup>1</sup> Visiting Astronomer at Cerro Tololo Inter-American Observatory (CTIO), which is operated by the Association of Universities for Research in Astronomy, Inc., under contract with the National Science Foundation.

$E(B-V) \sim 0.29$  and deduced a model-dependent lower limit on the mass of the compact object of  $10 M_{\odot}$ . Further excitement was provided by the discovery of a variable emission line near 500 keV, which is probably due to electron-positron annihilation (Sunyaev et al. 1992; Goldwurm et al. 1992).

With this assortment of facts and analogies in view, we conducted an optical study at CTIO of XN Mus 1991 in a quiescent state, 15 months after the nova outburst. The results provide dynamical evidence for the black hole hypothesis and strengthen the case for a close similarity between XN Mus 1991 and A0620-00.

## 2. OBSERVATIONS AND ANALYSIS

Spectral observations of XN Mus 1991 were obtained with the 4 m telescope at CTIO on 1992 April 3 (UT). The Ritchey-Chrétien spectrograph was used with the Reticon II CCD (1200 × 400 pixels) and the KPGL-3 grating, yielding  $\sim 4 \text{ \AA}$  resolution. The width of the entrance slit was  $1''.8\text{--}2''.2$ . Observing conditions were clear, with “seeing” between  $1''.6$  and  $3''.0$ . The slit was frequently rotated to maintain approximate alignment with the parallactic angle (Filippenko 1982). The quiescent optical counterpart ( $V \sim 20.5$ ) was clearly visible on the guider TV, when viewed with 15 s integration time. Twenty-one exposures (1200 s each) of XN Mus 1991 were interspersed with 12 exposures of wavelength calibration lamps (He-Ne-Ar). We observed flux standards and several dwarf stars (G, K, and M types) that have well-determined systemic velocities. Spectral reductions were performed at CTIO using the software package IRAF. The wavelength calibrations were interpolated dispersion solutions, scaled according to the time of an observation relative to the times of the lamp exposures. Cross-correlations between the flux-calibrated spectra of XN Mus 1991 and the velocity standards were computed for the range 4900–6500 Å, using two different software packages to confirm the results.

Photometric observations were made on both the 1.5 m telescope (1992 April 5–8) and the 0.9 m telescope (1992 April 3, 4, 6, 8, 14, and 15) at CTIO. Observations with the 1.5 m utilized the CFCCD camera and Tek No. CCD, along with a Corning No. 9780 filter (hereafter “ $B+V$ ”), which has a broad bandpass (FWHM = 2200 Å) centered at 4700 Å. Images from the 0.9 m telescope were obtained with both the TI No. 2 and Tek No. 1 CCDs, using two  $I$ -band filters (a standard  $I$  filter or a broad filter, Schott RG9/3). Images were processed to eliminate the electronic bias and correct for pixel-to-pixel sensitivity variations. The relative intensities of XN Mus 1991 and selected field stars were computed from minimum  $\chi^2$  fits to the point-spread function of each image using DAOPHOT (Stetson 1987) for the  $I$ -band data and similar software for the  $B+V$  data. The light curves were later calibrated to magnitude scales via standard photometric analyses (i.e., integrating the net counts within a  $10''$  aperture), performed for the designated “point-spread” stars and also selected standard stars of Landolt (1983).

## 3. SPECTRAL RESULTS

We used the spectra of the velocity standards as cross-correlation templates in an effort to derive a radial velocity curve for the secondary star. The 21 individual (1200 s) spectra of XN Mus 1991 were cross-correlated against each of the template stars. Comparable velocity curves were obtained with each template spectrum. The quality of the results, however, was judged to be best for the K0 V template star, HD 144179,

which yielded 15 unambiguous cross-correlation peaks ( $r > 2.6$ ; Tonry & Davis 1979). The six remaining spectra of XN Mus 1991 yielded  $r$ -values less than 2.3, which implies that the signal-to-noise ratio of absorption features was not sufficient to produce velocities with statistical significance greater than  $2.3 \sigma$ . The latter data, which were well distributed in time, were not used to derive any of the results reported in this Letter.

The 15 velocities derived using HD 144179 as a template star are shown in Figure 1. The results imply that the secondary star in XN Mus 1991 is orbiting a compact object with a velocity semi-amplitude greater than  $400 \text{ km s}^{-1}$ . The velocities of the secondary contrast sharply with the behavior of the night-sky lines (not shown) in the same 15 observations, which show an rms variation less than  $10 \text{ km s}^{-1}$ . Furthermore, the measured velocities of the template star (HD 26151, HD 42581, HD 51849, HD 144179, HD 154363, and IDS 16597) agree with the velocities given in the SIMBAD data base with an rms difference of  $11 \text{ km s}^{-1}$ .

The duration of spectral observations ( $\sim 9$  hr) is insufficient to determine a reliable orbital period, so we adopt the photometric period ( $P$ ) of 10.398 hr, which is fully documented below. Assuming a sine function, the velocities are best fitted ( $\chi^2_{\nu} = 1.20$ ) by the orbital parameters given in Table 1. The velocity semi-amplitude  $K$ , systemic velocity  $\gamma$ , and epoch of maximum redshift  $T_0(\text{spec})$  define the velocity ephemeris, which is represented by a solid line in Figure 1. The mass function may be derived from these results:

$$\frac{(M_x \sin i)^3}{(M_x + M_c)^2} = \frac{PK^3}{2\pi G} = 3.07 \pm 0.40 M_{\odot}.$$

There were no reported optical or X-ray eclipses during outburst (Bailyn 1992). Therefore, if the secondary is a  $0.7 M_{\odot}$  main-sequence star that fills its Roche lobe, then the inclination angle ( $i$ ) must be less than  $74^\circ$  for  $M_x \leq 3 M_{\odot}$ . If one considers the most favorable case that might admit the presence of a neutron star in the binary system, namely,  $i = 77^\circ$ , which implies that  $M_x$  is not less than  $4.45 \pm 0.46 M_{\odot}$ . Similarly, for an assumed  $0.3 M_{\odot}$  undermassive secondary, we find  $i < 80^\circ$ , and the corresponding mass limit is  $M_x = 3.75 \pm 0.43 M_{\odot}$ . Therefore, our results rule against a neutron star model at the  $2 \sigma$  confidence level, even with extreme values for  $i$  and the mass of the secondary. In the case of a  $0.7 M_{\odot}$  K star and a

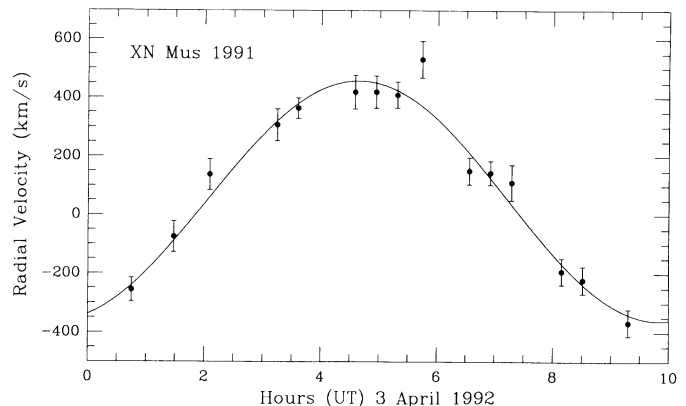


FIG. 1.—Radial velocity measurements of the secondary star in XN Mus 1991 (filled circles). Also plotted is the fitted curve, which assumes a circular orbit and the orbital period derived from CCD photometry (see Table 1 for parameter values).

TABLE 1  
ORBITAL PARAMETERS FOR XN MUS 1991

Parameter	Result
Orbital period (days) .....	$0.43325 \pm 0.00058$
$T_0$ (photometric, UT) .....	1992 April 3.5154 $\pm$ 0.0015
$T_0$ (photometric, heliocentric) .....	HJD 2,448,716.0179 $\pm$ 0.0015
$T_0$ (spectroscopic, UT) .....	1992 April 3.1933 $\pm$ 0.0029
$T_0$ (spectroscopic, heliocentric) .....	HJD 2,448,715.6958 $\pm$ 0.0029
$\gamma$ velocity ( $\text{km s}^{-1}$ ) .....	$48 \pm 17$
$K$ velocity ( $\text{km s}^{-1}$ ) .....	$409 \pm 18$
Mass function ( $M_\odot$ ) .....	$3.07 \pm 0.40$

more moderate inclination angle, e.g.,  $i = 60^\circ$ ,  $M_x = 5.92 \pm 0.62 M_\odot$ . For a great majority of the available parameter space (in  $K$ ,  $i$ , and  $M_c$ ), the compact object in XN Mus 1991 exceeds  $3 M_\odot$  and is very likely a black hole (Chitre & Hartle 1976).

The sum of the 15 spectra of XN Mus 1991 in the rest frame of the secondary star is shown in Figure 2. The spectrum of the template star, HD 144179, is also shown for comparison. Most of the stronger absorption lines of HD 144179 are evident in XN Mus 1991. The cross-correlation analysis favors the template star with spectral type K0; however, the relative absorption-line strengths of XN Mus 1991 and the continuum discontinuity at Mg  $b$  ( $\sim 5175 \text{ \AA}$ ) suggest a later spectral type,  $\sim K3$ . Given our limited signal-to-noise ratio, we conclude that the spectral type of the secondary star is in the range K0–K4. Since the orbital period and mass estimates imply a binary separation of 4–5  $R_\odot$ , the secondary is presumed to be luminosity class V.

The spectrum of XN Mus 1991 shows broad emission lines at H $\alpha$  and H $\beta$ , suggesting the presence of a residual accretion disk. In the individual exposures, the widths of the Balmer lines are in the range 1500–2500  $\text{km s}^{-1}$ , FWHM. The intensities and profiles appear highly variable and asymmetric; the interpretation of these complex data requires further analysis.

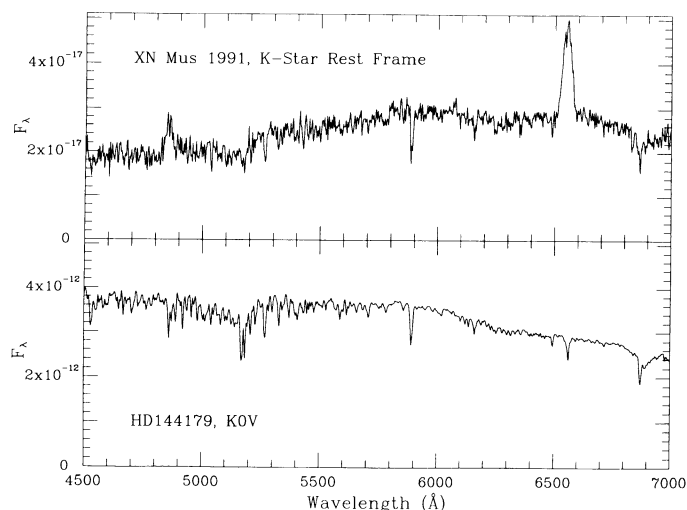


FIG. 2.—In the top panel is the spectrum of XN Mus 1991, Doppler-shifted to the rest frame of the secondary star but not dereddened [ $E(B-V) = 0.29$ ]. In the lower panel is the spectrum of HD 144179, which was used as a template for the cross-correlation analysis.

#### 4. PHOTOMETRY RESULTS

The relative light curves of XN Mus 1991 were derived in the manner described in § 2. We search for periodicity by computing the variance statistic of Stellingwerf (1978). For each trial period we folded the light curve into 50 phase bins and calculated the bin-averaged variance relative to the variance of the overall, unfolded light curve. Thus, a value near unity suggests an absence of periodic variations at that trial period, while a deep minimum is expected for a coherent modulation in brightness. Deep minima were obtained at  $10.380 \pm 0.017$  hr in the  $I$  band and  $10.430 \pm 0.031$  in the  $B+V$  band. We also conducted period searches using other techniques that utilize the measurement uncertainties, such as minimum  $\chi^2$  fits to a truncated Fourier series. In each case the most significant result occurred near 10.4 hr. We estimated the statistical uncertainty in the period determination using the Monte Carlo method described in Silber et al. (1992).

Since the folded light curves exhibited similar shapes in the  $B+V$  and  $I$  bands, we sought a more accurate period determination by normalizing all of the data to a single scale before computing the variance statistic. The 290 measurements in the  $B+V$  band are well distributed in phase, and we normalized these data by dividing by the mean value. The 165  $I$ -band measurements were collected using two different filters, and each data set requires a different normalization. The offset is 0.089 mag, which we believe is primarily due to the broad bandpass of the RG9/3 filter. The results for the range 3–15 hr are shown in Figure 3. The deepest minimum, at  $10.398 \pm 0.014$  hr, corresponds to a double-wave modulation with unequal maxima and minima; this is interpreted as the orbital period of XN Mus 1991. The other five minima in Figure 3 are explained by the shape of the light curve and the aliases expected from the daily sampling pattern. The period derived for XN Mus 1991 in quiescence is significantly shorter ( $9.8 \sigma$ ) than the period determined from the maximum number of elapse cycles ( $10.543 \pm 0.005$  hr) observed during outburst (Table 3 of Bailyn 1992). This result was predicted by the “superhump” model for the outburst variations.

Figure 4 shows the measurements in the  $B+V$  and  $I$  bands, folded at a period of 10.398 hr and displayed both individually and as phase-binned averages. Given the nonstandard nature of the  $B+V$  filter and the differences between the two  $I$ -band

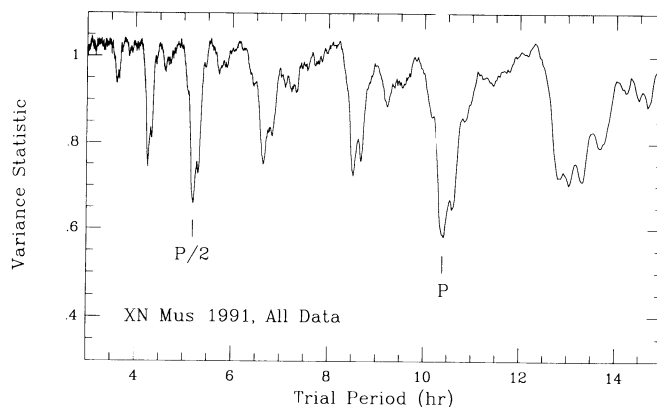


FIG. 3.—Period search for XN Mus 1991 using the combined light curve ( $B+V$  and  $I$  bands). The orbital period (10.398 hr; marked “P”) represents a double-wave modulation per orbital cycle. The minimum at 5.2 hr (marked “P/2”) corresponds to one-half the orbital period. The minima on either side of P and P/2 are 1 cycle count aliases of the P/2 modulation.

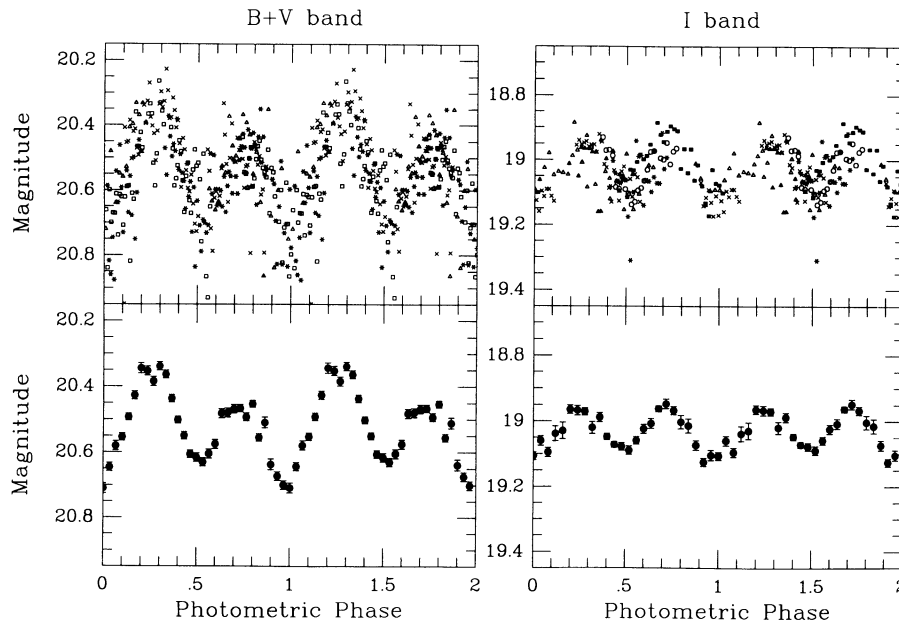


FIG. 4.—Folded light curves in the  $B+V$  and  $I$  bands. The  $B+V$  magnitudes are normalized approximately to the standard  $V$  band, since that portion of the  $B+V$  filter dominates the count rate. The upper panels show all of the individual data points. Observation dates and the symbol types correspond as follows:  $B+V$  measurements during April 5–8 are open triangles, open circles, crosses, and asterisks, respectively. The  $I$ -band display uses the same sequence of symbols for April 3, 4, 6, and 8; in addition, April 14 and 15 are shown as filled triangles and squares, respectively. The rms statistical errors, suppressed here in order to view the individual data points, are 0.045 mag in  $B+V$  and 0.037 mag in the  $I$  band. The lower panels contain phase-averaged results for the same data sets. Here the error bars are empirical uncertainties for the mean values found in each phase bin.

filters, the accuracy of the normalization to calibrated magnitudes is  $\sim 0.1$  mag. Comparing the different colors, it is clear that the modulation amplitude and the inequality of the maxima and minima are greater at shorter wavelength.

The photometric phase is defined by an optical minimum, choosing (if known) the one corresponding to the alignment of both stars along the line of sight, with the secondary star closer to the observer. Photometric phase zero is therefore equivalent to a spectroscopic phase of 0.75. The ephemerides for XN Mus 1991 (summarized in Table 1) are in agreement with these definitions, as the photometric and spectroscopic epochs differ in phase by  $0.744 \pm 0.008$ . Therefore, our interpretation that the optical light curves are dominated by ellipsoidal variations is supported by the timing of the brightness modulations relative to the radial velocities.

## 5. DISCUSSION

The hypothesis that XN Mus 1991 is a black hole binary is supported in two ways. First, the large value of the mass function and probable values of the inclination angle and the mass of the K star make it very likely that the mass of the compact object is greater than  $3 M_{\odot}$ . Second, there are strong similarities between XN Mus 1991 and the established black hole binary A0620–00, both during outburst and in quiescence. The similarity in the high-energy spectra and in the nova-decay light curves (X-ray and optical) suggests that these novae have common outburst mechanism and emission physics. We have now shown that the mass functions, secondary stars, orbital periods, quiescent light curves, and residual accretion disks are also very similar. X-ray spectral signatures have been helpful in identifying black hole candidates (White & Marshall 1984; Tanaka 1989). The most secure black holes (i.e., those based on dynamical studies of the secondary star) are Cyg X-1, LMC X-3, LMC X-1, A0620–00, V404 Cyg, and XN Mus 1991. All

six of these systems have exhibited a power-law X-ray component that may extend to hundreds of keV; all have additionally shown, at some time, an “ultrasoft” low-energy component below 2 keV (Tanaka 1989; Greiner et al. 1991). Moreover, these combined characteristics do not appear in X-ray pulsars and bursters, which contain neutron stars. Therefore, there is now greater justification for using X-ray spectral characteristics to identify black hole candidates when the spectrum of the secondary star cannot be measured (e.g., GX 339–4 and GS 2000+25).

The difference between outburst and quiescent optical periods in XN Mus 1991 was predicted by Bailyn (1992) on the basis of an interpretation that the outburst light curve was analogous to the “superhump” phenomenon in dwarf novae (see review by Warner 1985). These results promote recent efforts to model the outbursts of soft-spectrum X-ray transients as the consequence of accretion disk instability (e.g., Mineshige, Kim, & Wheeler 1990).

Despite the striking similarities between XN Mus 1991 and A0620–00, a few differences should be noted. The wavelength dependence of the light curves (Fig. 4) appears stronger in XN Mus 1991, while the amount of continuum emission provided by the accretion disk relative to the K star appears weaker in XN Mus 1991. The asymmetry in the  $B+V$  band near photometric phase 0.0 and the high maximum at photometric phase 0.25 suggest a bright spot in that quadrant of the binary plane. However, this is not the expected location of the “hot spot” caused by the impact between the accretion path and the outer edge of the disk (e.g., McClintock & Remillard 1990). Further analyses of the folded light curves and the spectral evidence of the disk are in progress.

We gratefully acknowledge the support provided by the staff at CTIO. We thank Nick Suntzeff for advice on using cross-

correlation software at CTIO, and Joyce Watson and the staff of the SIMBAD data base (Centre de Données Stellaires, Strasbourg, France) for help in selecting comparison stars. Partial

support for this work was provided by NSF grant AST 86-12572 and NASA grant NAGW-2469.

## REFERENCES

- Avni, Y. 1978, in *Physics and Astrophysics of Neutron Stars and Black Holes*, ed. R. Giacconi & R. Ruffini (Amsterdam: North-Holland), 43
- Bailyn, C. D. 1992, *ApJ*, 391, 298
- Bolton, T. 1975, *ApJ*, 200, 269
- Casares, J., & Charles, P. A. 1992, *MNRAS*, 255, 7
- Casares, J., Charles, P. A., & Naylor, T. 1992, *Nature*, 355, 614
- Cheng, F. H., Horne, K., Panagia, N., Shrader, C. R., Gilmozzi, R., Paresce, F., & Lund, N. 1992, *STScI preprint*
- Chitre, D. M., & Hartle, J. B. 1976, 207, 592
- Cowley, A. P., Crampton, D., Hutchings, J. B., Remillard, R., & Penfold, J. E. 1983, *ApJ*, 272, 118
- Della Valle, M., Jarvis, B. J., & West, R. M. 1991a, *A&A*, 247, L33
- . 1991b, *Nature*, 353, 50
- Filippenko, A. V. 1982, *PASP*, 94, 715
- Gies, D. R., & Bolton, C. T. 1986, *ApJ*, 304, 371
- Goldwurm, A., et al. 1992, *ApJ*, 389, L79
- Greiner, J., Egger, R., Hartner, G., Hasinger, G., & Pietsch, W. 1991, in *Proc. Workshop on Nova Muscae 1991* (Lyngby), ed. S. Brandt (Lyngby: Danish Space Research Inst.), 79
- Haswell, C. A., & Shafter, A. W. 1990, *ApJ*, 359, L47
- Johnston, H. M., Kulkarni, S. R., & Oke, J. B. 1989, *ApJ*, 345, 492
- Kesteven, M. J., & Turtle, A. J. 1991, *IAU Circ.*, No. 5181
- Landolt, A. U. 1983, *AJ*, 88, 439
- Lund, N., & Brandt, S. 1991, *IAU Circ.*, No. 5161
- Makino, F., et al. 1991, *IAU Circ.*, No. 5161
- McClintock, J. E., & Remillard, R. A. 1986, *ApJ*, 308, 110
- . 1990, *ApJ*, 350, 386
- Mineshige, S., Kim, S., & Wheeler, J. C. 1990, *ApJ*, 358, L5
- Silber, A., Bradt, H. V., Ishida, M., Ohashi, T., & Remillard, R. A. 1992, *ApJ*, 389, 704
- Stellingwerf, R. F. 1978, *ApJ*, 224, 953
- Stetson, P. 1987, *PASP*, 99, 191
- Sunyaev, R., et al. 1992, *ApJ*, 389, L75
- Tanaka, Y. 1989, in *Proc. 23d ESLAB Symp. (Bologna)*, ed. J. Hunt & B. Battrock (ESA SP-296; Noordwijk: ESA), 1, 3
- Tonry, J., & Davis, M. 1979, *AJ*, 84, 1511
- Warner, B. 1985, in *Interactive Binaries*, ed. P. P. Eggleton & J. E. Pringle (Dordrecht: Reidel), 367
- White, N. E., & Marshall, F. E. 1984, *ApJ*, 281, 354